



HAL
open science

Raman and infrared study of $(\text{PbO})_x (\text{P}_2\text{O}_5)_{(1-x)}$ glasses

Gwenn Le Saoût, Patrick Simon, Franck Fayon, Annie Blin, Yann Vaills

► **To cite this version:**

Gwenn Le Saoût, Patrick Simon, Franck Fayon, Annie Blin, Yann Vaills. Raman and infrared study of $(\text{PbO})_x (\text{P}_2\text{O}_5)_{(1-x)}$ glasses. *Journal of Raman Spectroscopy*, 2002, 33 (9), pp.740-746. 10.1002/jrs.911 . hal-03251325

HAL Id: hal-03251325

<https://hal.science/hal-03251325>

Submitted on 7 Jun 2021

HAL is a multi-disciplinary open access archive for the deposit and dissemination of scientific research documents, whether they are published or not. The documents may come from teaching and research institutions in France or abroad, or from public or private research centers.

L'archive ouverte pluridisciplinaire **HAL**, est destinée au dépôt et à la diffusion de documents scientifiques de niveau recherche, publiés ou non, émanant des établissements d'enseignement et de recherche français ou étrangers, des laboratoires publics ou privés.

Raman and infrared study of $(\text{PbO})_x(\text{P}_2\text{O}_5)_{(1-x)}$ glasses

Gwenn Le Saoût,* Patrick Simon, Franck Fayon, Annie Blin and Yann Vails

Centre de Recherche sur les Matériaux à Hautes Températures, CNRS, 1D avenue de la Recherche Scientifique, 45071 Orléans cedex 2, France

The structure of binary $(\text{PbO})_x(\text{P}_2\text{O}_5)_{(1-x)}$ glasses was investigated using Raman scattering and infrared spectroscopy, over the compositional range $x = 0.5\text{--}0.68$. The distribution of the phosphate groups $(\text{PO}_2)^-$, $(\text{PO}_3)^{2-}$, $(\text{P}_2\text{O}_7)^{4-}$ and $(\text{PO}_4)^{3-}$, determined from the simulation of Raman spectra in the $800\text{--}1500\text{ cm}^{-1}$ wavenumber range, indicates a significant disproportionation reaction near the pyrophosphate composition and shows a phosphorus connectivity scheme in the glass structure in agreement with ^{31}P magic angle spinning NMR results. The low-wavenumber Raman spectra of glasses are discussed in the light of the spectra of crystals. The mode laying in the far-infrared region and due to lead–oxygen vibrations exhibits a composition-dependent wavenumber that correlates with bulk glass properties such as glass transition temperature.

INTRODUCTION

The recently developed lead phosphate-based glasses have high thermal expansion coefficients and exhibit interesting optical properties. These properties make them attractive for a variety of applications including hermetic seals to high-expansion metals and visible and infrared optical components.¹ Hence the characterization and understanding of their structure on different length scales is desirable but remains experimentally difficult, mainly owing the lack of periodicity inherent to glasses. Only the combination of the results of several methods gives insight into the glass structure. Infrared and Raman spectroscopic techniques are suitable methods for investigating phosphate glasses and allow an easy and fruitful comparison.²

In phosphate glasses, phosphorus always stands in tetrahedral coordination. As for silicates and aluminosilicates, the different tetrahedra can be classified according to their connectivities, Q_n , where n is the number of bridging oxygen atoms per PO_4 tetrahedron. However, most research on the vibrational spectroscopy of phosphate crystals compounds treat information on their structure in terms of oxygen bridges and terminal groups rather than in terms of Q_n species.³ It is known that both the polar and non-polar vibrations characteristic of phosphate lattices are active in both IR and Raman spectra. The IR spectra are dominated by intense bands related to cation vs anion mode variations whereas the Raman spectra are dominated by intense bands related to modes involving polarizability variations. Generally the assignment of modes in the glasses is done by reference

to what is known in the crystalline phases of equivalent composition.³ In this work, Raman spectra of lead phosphate glasses and crystals were obtained and compared with each other. This comparison of IR and Raman spectra was done to improve the band assignments. A systematic deconvolution of Raman spectra into basic components was done in order to monitor quantitatively the structural changes of such glasses. The results are compared with those of ^{31}P magic angle spinning nuclear magnetic resonance (MAS NMR) spectroscopy.⁴

Intense bands observed in far-IR ($0\text{--}300\text{ cm}^{-1}$) spectra are assigned to localized vibrations of cations in the glass. Observation of these bands provides a method for directly probing the interaction forces between ions and their neighbouring environment in glasses.⁵ In binary lead phosphate glasses, we compared the lead local environment deduced from far-IR results and that previously probed by EXAFS,⁶ x-ray diffraction⁷ and ^{207}Pb NMR.⁸ Low-wavenumber Raman scattering ($0\text{--}200\text{ cm}^{-1}$) is also of interest and the so-called boson peak may be used to extract intermediate-range structural information in amorphous materials.⁹

EXPERIMENTAL

The $(\text{PbO})_x(\text{P}_2\text{O}_5)_{(1-x)}$ samples were prepared from stoichiometric powders resulting from the mixing of $(\text{NH}_4)_2\text{HPO}_4$ and $\text{Pb}(\text{NO}_3)_2$ aqueous solutions ($x = 0.5, 0.55, 0.6, 0.66$ and 0.68). The mixtures were melted in Pt crucibles for 1 h at temperatures varying from 700 to 850°C depending on composition and the melt was poured on to a stainless-steel slab. All sample compositions were checked by chemical analysis (1 mol% uncertainties). For IR experiments, the glass samples were polished using ethanol and

*Correspondence to: Gwenn Le Saoût, Centre de Recherche sur les Matériaux à Hautes Températures, CNRS, 1D avenue de la Recherche Scientifique, 45071 Orléans cedex 2, France.
E-mail: lesaout@cnrs-orleans.fr

opaline at the final stage, except for the $x = 0.68$ material, which was too thin to be polished without destroying it (thickness = 0.7 mm). Crystalline $\text{Pb}(\text{PO}_3)_2$, $\text{Pb}_3\text{P}_4\text{O}_{13}$ and $\text{Pb}_2\text{P}_2\text{O}_7$ were obtained by annealing the glasses with same composition at 500°C and were checked by powder x-ray diffraction.

Glass transition temperatures were determined by differential scanning calorimetry (DSC, Setaram 92) at a heating rate of 5°C min^{-1} .

Raman spectra were recorded on a Jobin-Yvon T 64000 spectrometer using 514.5 nm radiation from a Coherent Innova 70 Spectrum argon–krypton ion laser. Detection was performed with a cooled charge-coupled device (CCD) multichannel detector. Measurements were carried out in a micro-Raman configuration (Olympus BX40 microscope); the laser power focused on the sample was about 0.4 W for the laser output. In order to eliminate the temperature and ω^4 scattering dependences, we always present the reduced intensity, I_{RED} , obtained from

$$I_{\text{RED}}(\omega) = I(\omega) \frac{1}{[1 + n(\omega)](\omega_0 - \omega)^4} \quad (1)$$

where $I(\omega)$ is the Raman intensity and $n(\omega)$ is the Bose–Einstein population factor.

Infrared reflectivity spectra were recorded near normal incidence using a Fourier transform scanning interferometer (Bruker IFS 113v), covering the wavenumber range $10\text{--}12\,000\text{ cm}^{-1}$ with an effective spectral resolution of 6 cm^{-1} . The wavenumbers of the transverse optical (TO) and longitudinal optical (LO) vibration modes were determined by fitting the IR reflectivity spectra with a four-parameter dielectric function model.¹⁰

RESULTS AND DISCUSSION

It is useful to divide the Raman and IR spectra into two regions ($600\text{--}1500$ and $0\text{--}600\text{ cm}^{-1}$) and to consider each region separately. Owing to the resulting vibrational interactions and band overlapping, characteristic features of the phosphate network are restricted to the high-wavenumber part of the spectrum ($600\text{--}1500\text{ cm}^{-1}$), corresponding to the stretching vibrations of the anions.²

Raman and IR spectra in the $600\text{--}1500\text{ cm}^{-1}$ wavenumber range

The Raman spectra of the crystalline compounds $\text{Pb}(\text{PO}_3)_2$, $\text{Pb}_3\text{P}_4\text{O}_{13}$, $\text{Pb}_2\text{P}_2\text{O}_7$, $\alpha\text{-Pb}_3(\text{PO}_4)_2$ and five polyphosphate glasses ranging in composition from $(\text{PbO})_{0.5}(\text{P}_2\text{O}_5)_{0.5}$ to $(\text{PbO})_{0.68}(\text{P}_2\text{O}_5)_{0.32}$ are displayed in Fig. 1.

Raman spectra of crystals

The bands are assigned by using the crystallographic data for the compounds and literature data on the wavenumber ranges related to the corresponding vibrations of structural groups in various crystalline phosphates.^{2,3}

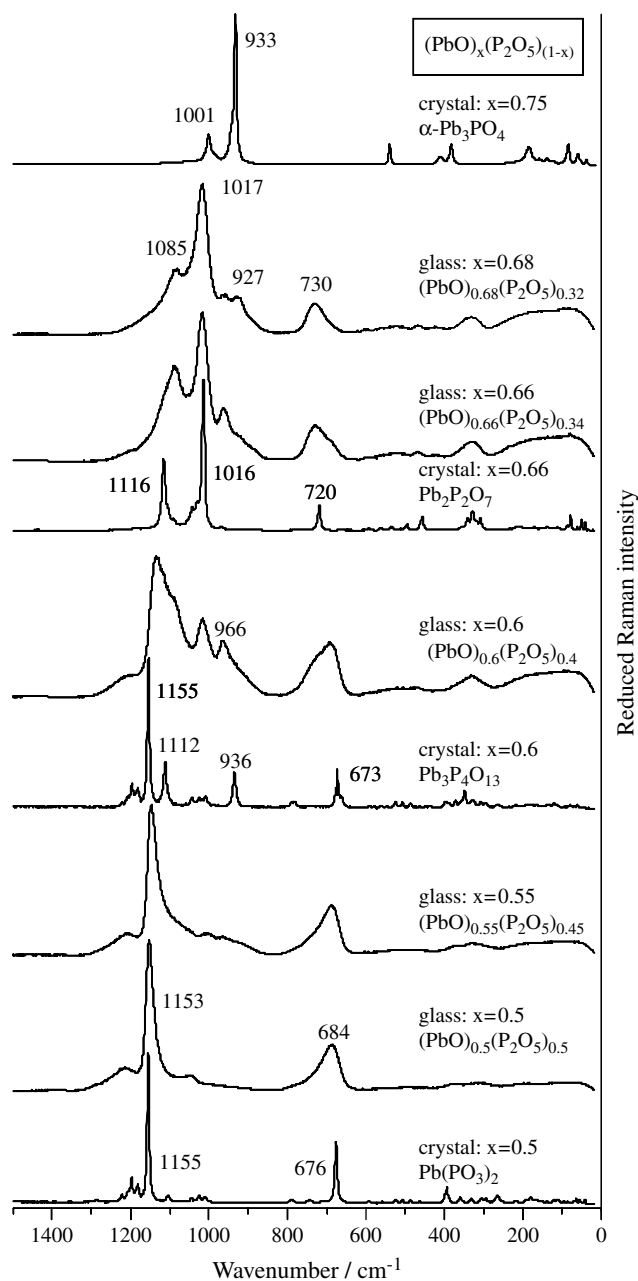


Figure 1. Reduced Raman spectra of the crystals and glasses in the system $(\text{PbO})_x(\text{P}_2\text{O}_5)_{(1-x)}$.

The structure of crystalline lead metaphosphate, $\text{Pb}(\text{PO}_3)_2$ ($x = 0.5$), consists of linear chains made of connected PO_4 tetrahedra.¹¹ The PO_4 tetrahedra are present as a middle chain group with two bridging oxygen atoms and two non-bridging oxygen atoms (Q_2 species). The $\text{Pb}(\text{PO}_3)_2$ Raman spectrum shows a pattern typical of the metaphosphate composition.² The sharp band at 1155 cm^{-1} is the dominant feature and has been assigned following Bobovich¹² to the symmetric stretching vibration of the two non-bridging oxygen ions bonded to phosphorus (PO_2^-). The band at

676 cm^{-1} is attributed to a symmetric P–O–P mode typical of condensed phosphates.¹²

In the crystalline lead tetrapolyphosphate $\text{Pb}_3\text{P}_4\text{O}_{13}$ ($x = 0.6$), the anion $(\text{P}_4\text{O}_{13})^{6-}$ is built up by four corner-sharing PO_4 tetrahedra (Q_2 and Q_1 species).¹³ The bands at 1112 and 1155 cm^{-1} are attributed to $\nu_s(\text{PO}_2)^-$ vibrations (Q_2 species) and the band at 936 cm^{-1} may be attributed to $(\text{PO}_3)^{2-}$ vibrations (Q_1 species).² The symmetric P–O–P mode is present at 673 cm^{-1} .

The structure of crystalline lead pyrophosphate, $\text{Pb}_2\text{P}_2\text{O}_7$ ($x = 0.66$), is composed of $(\text{P}_2\text{O}_7)^{4-}$ anions (Q_1 species).¹⁴ The essential features of the vibrational spectrum of the $(\text{P}_2\text{O}_7)^{4-}$ anions are the bands at 1016 and 1116 cm^{-1} attributed to symmetric $\nu_s(\text{P}_2\text{O}_7)^{4-}$ vibrations and the band at 720 cm^{-1} attributed to $\nu_s(\text{P–O–P})$.¹⁵

The structure of the lead orthophosphate crystal α - $\text{Pb}_3(\text{PO}_4)_2$ ($x = 0.75$) is made of isolated $(\text{PO}_4)^{3-}$ ions (Q_0 species).¹⁶ The bands at 933 and 1001 cm^{-1} are attributed to the A_g modes of the $(\text{PO}_4)^{3-}$ ion according to Benoit and Chapelle.¹⁷ As expected, P–O–P vibrations are absent.

Raman and IR spectra of glasses

In the range 600–1500 cm^{-1} , five dominant features are present in the Raman spectra at about 684, 927, 966, 1017 and 1213 cm^{-1} . From the comparison between the glass spectra and those of crystalline compounds of known structure, these bands are assigned to the $\nu_s(\text{P–O–P})$, $\nu_s(\text{PO}_4)^{3-}$, $\nu_s(\text{PO}_3)^{2-}$, $\nu_s(\text{P}_2\text{O}_7)^{4-}$ and $\nu_s(\text{PO}_2)^-$ vibrations, respectively. The Raman spectra reveal that the $(\text{PbO})_{0.5}(\text{P}_2\text{O}_5)_{0.5}$ glass is composed of $(\text{PO}_2)^-$ middle chain groups, whereas the number of $(\text{P}_2\text{O}_7)^{4-}$ and $(\text{PO}_4)^{3-}$ species increases with increasing PbO content. The variation of the Raman spectra is similar to those reported for $\text{MO–P}_2\text{O}_5$ glasses with $\text{M} = \text{Li}$ ¹⁸ and $\text{M} = \text{Zn}$,¹⁹ and shows progressive depolymerization of the phosphate network with increasing modifier cation concentration. We can note in the Raman spectra for the glass compositions $(\text{PbO})_{0.5}(\text{P}_2\text{O}_5)_{0.5}$ and $(\text{PbO})_{0.55}(\text{P}_2\text{O}_5)_{0.45}$ the presence of a weak shoulder at about 1290 cm^{-1} attributed to P=O vibrations (Q_3 species).²⁰

Figure 2 shows the imaginary parts of the dielectric (TO-mode structure) and the inverse dielectric (LO-mode structure)

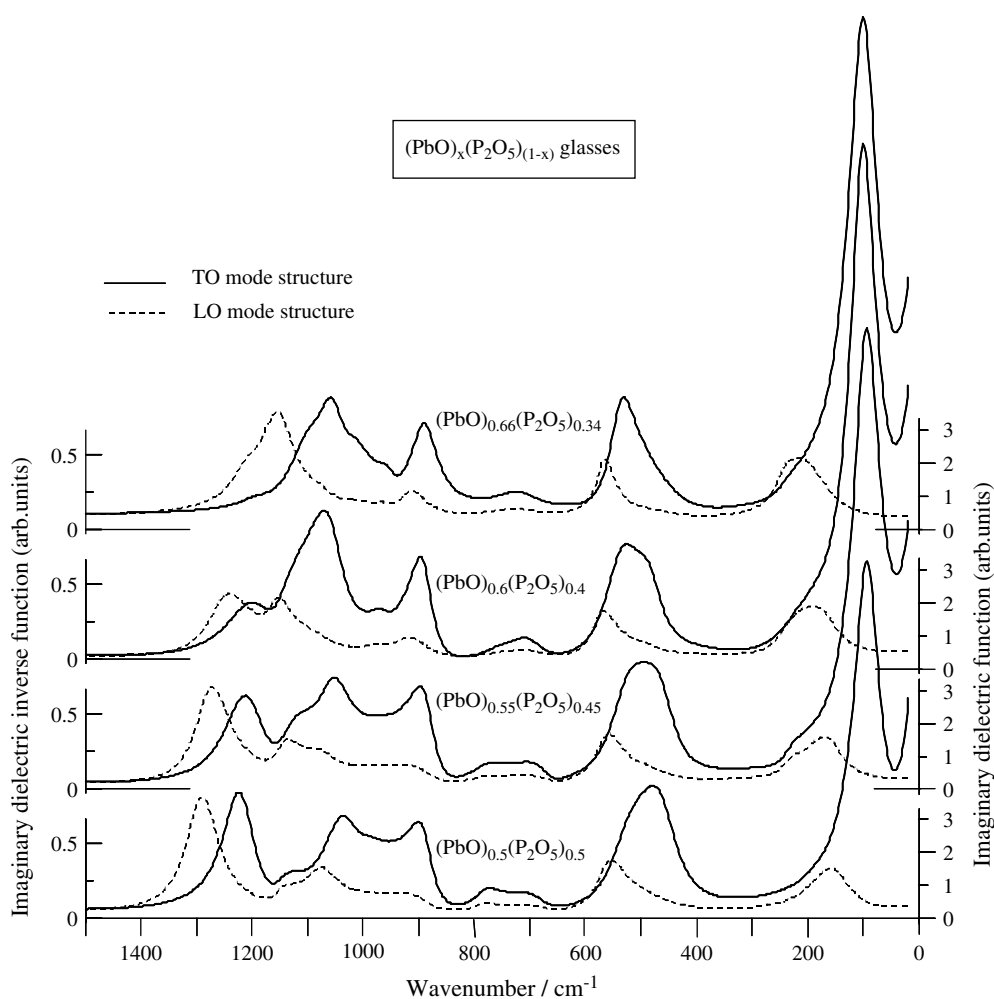


Figure 2. Imaginary parts of the dielectric (solid lines) and the inverse dielectric (dashed lines) functions of the $(\text{PbO})_x(\text{P}_2\text{O}_5)_{(1-x)}$ glasses.

Table 1. Wavenumber ranges of the IR bands related to the vibrations of various phosphate groups³

Structural group	Wavenumber ranges of feature locations/cm ⁻¹	
	Crystals	Glasses
P–O–P bridge	850–1060	840–1050
(PO ₄) ³⁻ anion	980–1100	980–1020
(PO ₃) ²⁻ end of chain	1030–1230	1080–1170
(PO ₂) ⁻ middle of chain	1140–1320	1080–1330

structure) functions obtained from IR reflectivity spectra in the 0–1500 cm⁻¹ range. Bands are less resolved than in the Raman spectra, implying a more difficult assignment. This originates from more coupled modes due to longer range interaction. Literature data available on these wavenumber ranges related to the corresponding vibrations of the structural groups in various crystalline and glass phosphates are presented in Table 1. For the (PbO)_{0.5}(P₂O₅)_{0.5} glass, the main IR bands can be assigned as follows: $\nu_{\text{as}}(\text{PO}_2)^-$, 1221 cm⁻¹; $\nu_{\text{as}}(\text{PO}_3)^{2-}$, 1045 cm⁻¹; and $\nu_{\text{as}}(\text{P–O–P})$, 887 cm⁻¹. The very strong band at 1221 cm⁻¹ is especially meaningful, as it is due to the asymmetric stretching vibration of the middle-chain units, which predominate in the metaphosphate structure. This vibration is also clearly present in the Raman spectrum. For the pyrophosphate glass (PbO)_{0.66}(P₂O₅)_{0.34}, the main bands wavenumbers can be assigned as follows: $\nu_{\text{as}}(\text{PO}_3)^{2-}$, 1056 cm⁻¹; and $\nu_{\text{as}}(\text{P–O–P})$, 890 cm⁻¹. The concentration of (PO₃)²⁻ groups increases when the long chains of a metaphosphate are replaced by the small pyrophosphate units. Using the comparison

of infrared and Raman spectra, a complete assignment is given in Table 2.

Band deconvolution of Raman spectra

A number of studies have used curve-fitting techniques to separate unresolved bands into several components (see, for example, Refs 21 and 22 and references cited therein). In disordered systems, a distribution of individual geometries exists, which results in a distribution of vibrational wavenumbers. At the same time, a vibrational coupling with some degree of coherence between vibrating units is expected, which also affect the observed band shape. In most studies the component Raman bands have been approximated by Gaussian functions. In order that the fit be as realistic as possible, we used in the first stage a minimum number of bands corresponding to the number of distinct features observed in the experimental spectrum such as resolved maxima and well developed shoulders. To improve the fit, we added in the second stage weaker bands obeying the following criteria: (i) the IR spectrum revealed an asymmetric mode that could be present in the Raman spectrum [e.g. $\nu_{\text{as}}(\text{PO}_2)^-$]; and (ii) we take into account the structural groups present in smaller quantities for a composition but in large quantities for another one. Figure 3 presents the band deconvolution of Raman spectra for (PbO)_{0.5}(P₂O₅)_{0.5}, (PbO)_{0.6}(P₂O₅)_{0.4} and (PbO)_{0.68}(P₂O₅)_{0.32} glasses in the 800–1400 cm⁻¹ spectral region. In this wavenumber range that corresponds to stretching vibrations, all Raman intensities can be directly compared. By deconvoluting the Raman spectra, the position and the relative intensity of each component band related to a vibrational mode of a phosphate structural group were determined. Only a weak band at about 1000 cm⁻¹ was not attributed. We can deduce the relative population of (PO₂)⁻,

Table 2. Raman and IR wavenumbers (cm⁻¹) and band assignments in the 600–1500 cm⁻¹ range for (PbO)_x(P₂O₅)_(1-x) glasses (weak intensities are in italics)

Wavenumber/cm ⁻¹									
<i>x</i> = 0.5		<i>x</i> = 0.55		<i>x</i> = 0.6		<i>x</i> = 0.66		<i>x</i> = 0.68	
R	IR	R	IR	R	IR	R	IR	R	Assignment
684	687–689	686	674	686	699–705	689	721–730	684	$\nu_{\text{s}}(\text{P–O–P})$
719	784–788	723	786–788	727	755–758	731		730	
774		773		774					
907	887–897	913	883–893	887	889–909	887	890–914	887	$\nu_{\text{as}}(\text{P–O–P})$
968		967		926		926		927	$\nu_{\text{s}}(\text{PO}_4)^{3-}$
		1018		966		965		965	$\nu_{\text{s}}(\text{PO}_3)^{2-}$
		1049	1057–1071	1017		1017		1017	$\nu_{\text{s}}(\text{P}_2\text{O}_7)^{4-}$
1049	1045–1076	1055		1049	1057–1073	1049	1056–1079	1049	$\nu_{\text{as}}(\text{PO}_3)^{2-}$
1133		1115		1088		1088		1085	$\nu_{\text{s}}(\text{PO}_2)^-$, (P ₂ O ₇) ⁴⁻
					1153–1156		1103–1155		$\nu_{\text{as}}(\text{PO}_3)^{2-}$
1153	1148–1151	1147	1142–1147	1133		1132		1132	$\nu_{\text{s}}(\text{PO}_2)^-$
1213	1221–1293	1209	1210–1278	1198	1196–1251	1172	1200–1206	1167	$\nu_{\text{as}}(\text{PO}_2)^-$
1288		1266							$\nu_{\text{s}}(\text{P=O})$

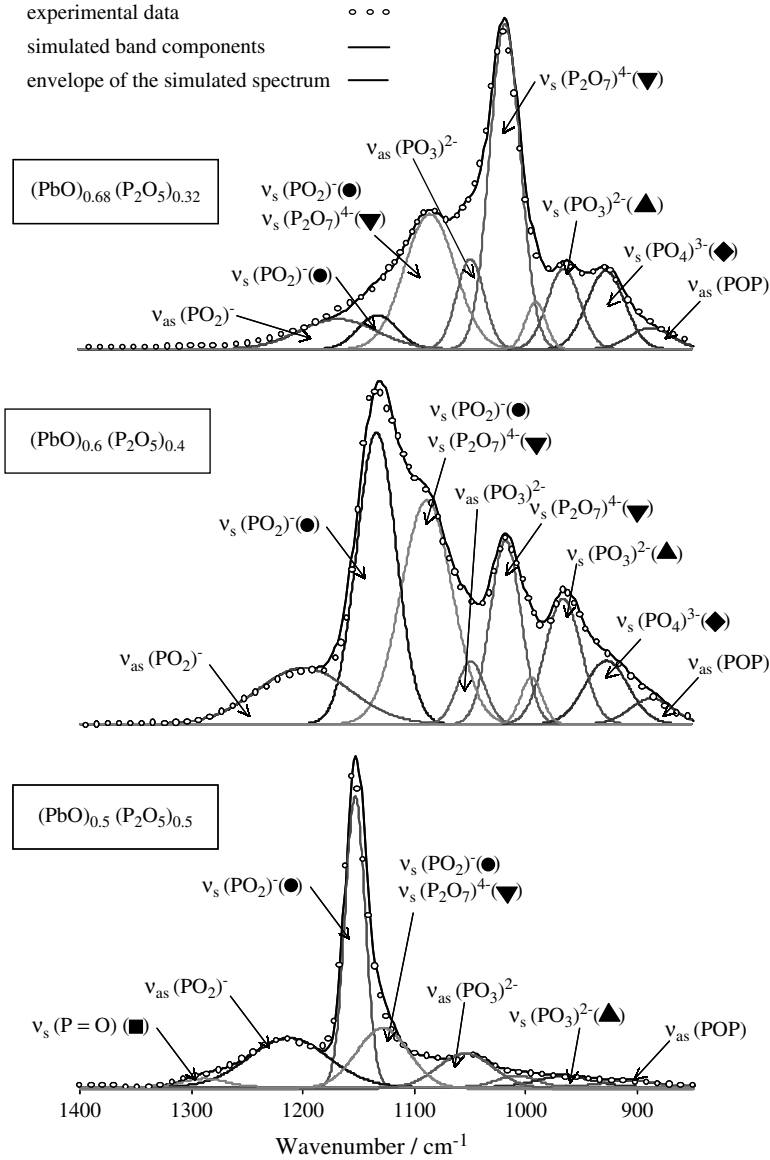


Figure 3. Band deconvolution of Raman spectra for glasses $(\text{PbO})_{0.5}(\text{P}_2\text{O}_5)_{0.5}$, $(\text{PbO})_{0.6}(\text{P}_2\text{O}_5)_{0.4}$ and $(\text{PbO})_{0.668}(\text{P}_2\text{O}_5)_{0.332}$ in the spectral region $800\text{--}1400\text{ cm}^{-1}$.

$(\text{PO}_3)^{2-}$, $(\text{P}_2\text{O}_7)^{4-}$ and $(\text{PO}_4)^{3-}$ structural groups species associated with Q_2 , Q_1 , $2Q_1$ and Q_0 species, respectively.

Figure 4 shows the variation of the Q_n populations determined from the simulation of the experimental Raman spectra, and also reported is the distribution previously determined by Fayon *et al.*⁴ from the simulation of 1D MAS NMR spectra. This description of the glass structure is limited to the short-range order, but the Raman spectra revealed $(\text{P}_2\text{O}_7)^{4-}$ anions that describe partially the Q_n connectivity scheme. Using solid-state ^{31}P MAS and 2D double quantum NMR, Fayon *et al.*⁴ also characterized the phosphorus connectivity scheme and determined quantitatively the $Q_{n,i}$ species, where the additional subscript i describes the type of bonded PO_4 group²³ [the $Q_{1,1}$ group is related to the

$(\text{P}_2\text{O}_7)^{4-}$ anion]. Figure 4 also shows the variation of the $Q_{1,1}$ populations determined by ^{31}P NMR⁴ and Raman spectroscopy. The results are in good agreement and valid the quantitative aspect for the Raman spectra at these compositions. We calculated the equilibrium constants k_n ($n = 1, 2$) of the disproportionation reactions²⁴



The equilibrium constants obtained are $k_2 = 0.002 \pm 0.002$ and $k_1 = 0.020 \pm 0.010$. For glasses having a PbO content close to 50 mol%, the Q_n distribution is close to a binary distribution ($k_2 \approx 0$), as expected for an ionic modifier cation.²⁴ However, the equilibrium constant calculated for

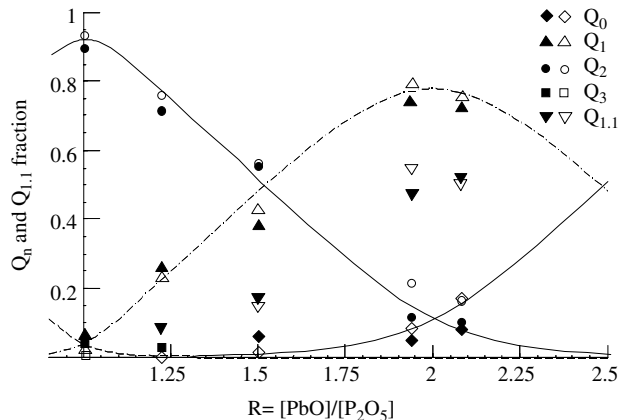


Figure 4. Experimentally determined Q_n and $Q_{1,1}$ distribution in lead phosphate glasses as a function of the $[\text{PbO}]/[\text{P}_2\text{O}_5]$ ratio by ^{31}P NMR (open symbols)⁴ and Raman (solid symbols) spectroscopy. The fitted lines were calculated from the equilibrium constant $k_2 = 0.002$ and $k_1 = 0.020$.

the disproportionation of the Q_1 species indicates a more random configuration of bridging and non-bridging oxygen atoms as the lead content increases. This variation is most often associated with glasses that contain high field strength modifying cations, consistent with Van Wazer's prediction²⁵ that phosphate melts with more covalent metal oxides will have a higher equilibrium constant for the disproportionation of the Q_1 species. This variation can be attributed to the appearance of more covalent Pb—O bonds in the glass structure. It should be noted that these equilibrium constants are very similar to those determined in zinc phosphate glasses¹⁹ and $\text{PbO}_x(\text{ZnO})_{(0.6-x)}(\text{P}_2\text{O}_5)_{0.4}$ glasses.²⁶

Low-wavenumber Raman spectra and far-IR spectra (0–200 cm^{-1})

Low-wavenumber Raman spectra

We can note in Fig. 1 the high intensity of the low-wavenumber Raman spectra of lead phosphate glasses compared with silica glass. This feature seems characteristic of glasses containing heavy metal oxides such as Tl_2O , PbO , BiO_2 , Sb_2O_3 ²⁷ or TeO_2 .²⁸ According to Lines *et al.*,²⁹ the well-known boson peak located in the wavenumber range 50–100 cm^{-1} , overlaps another contribution at about 70–160 cm^{-1} attributable to a mode dominated by the motion of the heavy metals.

VH and VV Raman spectra of the $(\text{PbO})_{0.68}(\text{P}_2\text{O}_5)_{0.32}$ glass and $\text{Pb}_2\text{P}_2\text{O}_7$ crystal are compared in Fig. 5. The intensities of the VV spectra of crystal and glass are normalized on the peak at 1016 cm^{-1} . The dominant feature in the low-wavenumber range of the Raman spectra of the glasses is a broad, asymmetric VH Raman band at about 55 cm^{-1} , seen also as a shoulder in the corresponding VV spectrum which shows a strong peak at about 85 cm^{-1} . The intensities of both of these bands grow with increasing Pb content (Fig. 1).

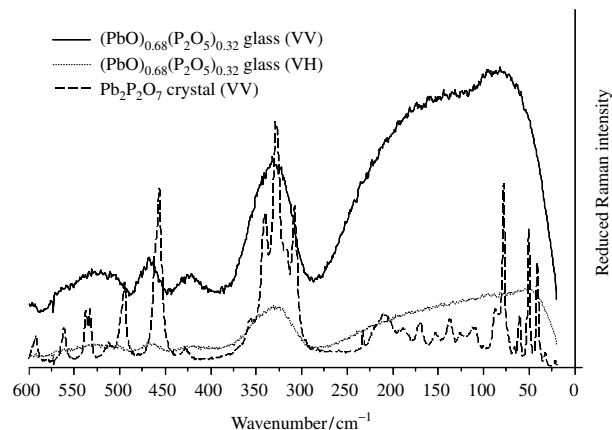


Figure 5. Reduced Raman spectra of $\text{Pb}_2\text{P}_2\text{O}_7$ crystal (VV polarization) and $(\text{PbO})_{0.68}(\text{P}_2\text{O}_5)_{0.32}$ glasses (VV and VH polarization).

The asymmetric band at 55 cm^{-1} in the VH spectra can be modelled by using a log-normal distribution, which seems to be a universal property of the boson peak.³⁰ However, contributions of Pb-connected lattice vibrations in the same spectral range render its unambiguous identification impossible, as was previously noted by Sigaev *et al.*³¹ in lead germanate glasses. We do not observe any significant change in its position with lead content. According to Zahra *et al.*,³² the narrow band at 120–140 cm^{-1} in the Raman spectra of lead silicate, lead borate and lead gallate glasses is due to the Pb—O vibrations either in PbO_4 square pyramids or in PbO_3 trigonal pyramids (with Pb atoms at the apex). The band at about 80–110 cm^{-1} is connected with higher coordinated Pb atoms.^{31,32} In our spectra, only the band at 80–100 cm^{-1} is clearly present. As displayed in Fig. 5, the Raman spectra of $\text{Pb}_2\text{P}_2\text{O}_7$ crystal and of $(\text{PbO})_{0.68}(\text{P}_2\text{O}_5)_{0.32}$ glass are well correlated in the whole range 20–600 cm^{-1} . Lead atoms in the $\text{Pb}_2\text{P}_2\text{O}_7$ crystal are eight- and nine-coordinated to oxygen atoms¹⁴ and give rise to the band at 85 cm^{-1} also present in the glass spectra.

Far-IR spectra

Intense bands observed in far-IR (0–300 cm^{-1} , Fig. 2) spectra are assigned to vibrations of Pb^{2+} cation at localized sites in the glass.⁵ We can observe an increase in the TO and LO wavenumbers with increasing lead content (from 96–160 cm^{-1} for $x = 0.5$ to 108–184 cm^{-1} for $x = 0.66$). According to the harmonic oscillator model, this variation can be related to an increase in the Pb—O force constant with increasing lead content. Exarhos³³ argues that the force constant is related to the bulk glass properties such as glass transition temperature and we can effectively observe an increase in the glass transition temperature with increasing lead content (Fig. 6).

By using a simplified version of the Born–Mayer potential, Nelson and Exarhos³⁴ obtained in phosphate glasses a correlation between the observed cation vibrational

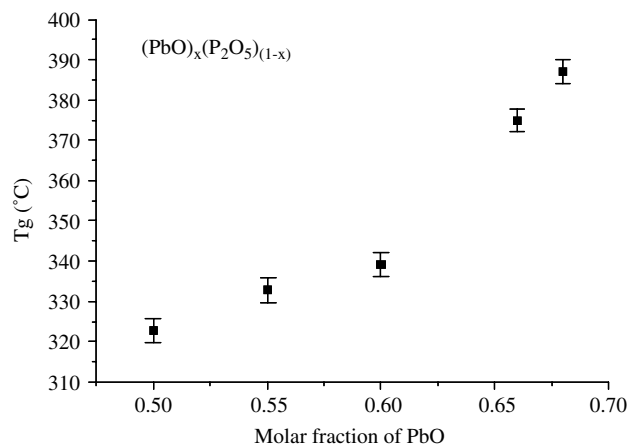


Figure 6. Variation of the glass transition temperature with lead content in $(\text{PbO})_x(\text{P}_2\text{O}_5)_{(1-x)}$ glasses.

wavenumber and the inverse of the cation oxygen inter-nuclear distance. The increase in TO and LO wavenumbers as the lead content increases can be explained by a decrease in the lead–oxygen distance. Low-wavenumber Raman and far-IR results show that the Pb atom has a high coordination number (>4) and that the Pb–O distances decrease as the lead content increases, consistent with the values of the k_n disproportionation constants previously obtained. These conclusions are in good agreement with the data on the local lead environment previously probed by EXAFS,⁶ x-ray diffraction⁷ and ²⁰⁷Pb NMR,⁸ which reveal an average coordination number between 7 and 10 and a decrease in Pb–O distances with increasing lead content.

CONCLUSION

Using Raman scattering and IR spectroscopy, we have investigated the structure of binary $(\text{PbO})_x(\text{P}_2\text{O}_5)_{(1-x)}$ glasses over the compositional range $x = 0.5–0.68$. The band deconvolution analysis of Raman spectra in the wavenumber range $800–1400\text{ cm}^{-1}$ allows one to follow quantitatively the structural changes as a function of the glass composition. We observe depolymerization of the phosphate network with increasing lead content. The results indicate a significant disproportionation reaction near the pyrophosphate composition which is attributed to the appearance of more covalent Pb–O bonds in the glass structure. The low-wavenumber Raman and far-IR results reveal a coordination number of the lead atom >4 and a decrease in the Pb–O distance as the lead content increases.

Acknowledgement

We thank Professor Yves Luspain for providing good quality single crystals of $\text{Pb}_3(\text{PO}_4)_2$.

REFERENCES

- Guo G. *Glass Technol.* 1998; **39**: 138.
- Rulmont A, Cathay R, Liegeois-Duyckaerts M, Tarte P. *Eur. J. Solid Inorg. Chem.* 1991; **28**: 207.
- Efimov E. *J. Non-Cryst. Solids* 1997; **209**: 209.
- Fayon F, Bessada C, Coutures JP, Massiot D. *Inorg. Chem.* 1999; **38**: 5212.
- Exarhos GJ, Miller PJ, Risen WM. *J. Chem. Phys.* 1974; **60**: 4145.
- Greaves GN, Gurman SJ, Gladden LF, Spence CA, Cox P, Sales BC, Boatner LA, Jenkins RN. *Philos. Mag. B* 1988; **58**: 271.
- Lai A, Musinu A, Piccaluga G, Puligheddu S. *Phys. Chem. Glasses* 1997; **38**: 173.
- Fayon F, Bessada C, Douy A, Massiot D. *J. Magn. Reson.* 1999; **137**: 116.
- Terki F, Levelut C, Boissier M, Pelous J. *Phys. Rev. B* 1996; **53**: 2411.
- Gervais F. In *Infrared and Millimeter Waves*, vol. 8. Button KJ (ed.). Academic Press: New York, 1983; 279.
- Jost KH. *Acta Crystallogr.* 1964; **17**: 1539.
- Bobovich YS. *Opt. Spectrosc.* 1962; **13**: 274.
- Averbuch-Pouchot MT, Durif A. *Acta Crystallogr., Sect. C* 1987; **43**: 631.
- Mullica DF, Perkins HO, Grossie DA, Boatner LA, Sales BC. *J. Solid State Chem.* 1986; **62**: 371.
- Stranford GT, Condrate RA, Cornilsen BC. *J. Mol. Struct.* 1981; **73**: 231.
- Keppeler U. *Z. Kristallogr.* 1970; **132**: 228.
- Benoit JP, Chappelle JP. *Solid State Commun.* 1974; **15**: 531.
- Tatsumisago M, Kowada Y, Minami T. *Phys. Chem. Glasses* 1988; **29**: 63.
- Brow RK, Tallant DR, Myers ST, Phifer CC. *J. Non-Cryst. Solids* 1995; **191**: 45.
- Meyer K. *J. Non-Cryst. Solids* 1997; **209**: 227.
- McMillan P. *Am. Mineral.* 1984; **69**: 622.
- Efimov E. *J. Non-Cryst. Solids* 1999; **253**: 95.
- Witter R, Hartmann P, Vogel J, Jäger C. *Solid State NMR* 1998; **13**: 189.
- Parks JR, Van Wazer JR. *J. Am. Ceram. Soc.* 1957; **79**: 4890.
- Van Wazer JR. *Phosphorus and Its Compounds*, vol. 1. Interscience: New York, 1958.
- Le Saoût G, Fayon F, Bessada C, Simon P, Blin A, Vaills Y. *J. Non-Cryst. Solids* 2001; **293–295**: 657.
- Miller AE, Nassau K, Lyons KB, Lines ME. *J. Non-Cryst. Solids* 1988; **99**: 289.
- Duverger C, Romain F, Khatir S, Bouzaoui M, Turrell S. *J. Mol. Struct.* 1997; **410–411**: 285.
- Lines ME, Miller AE, Nassau K, Lyons KB. *J. Non-Cryst. Solids* 1987; **89**: 163.
- Pocsik I, Koos M. *Solid State Commun.* 1990; **74**: 1253.
- Sigaev VN, Gregora I, Pernice P, Champagnon B, Smelyanskaya EN, Aronne A, Sarkisov PD. *J. Non-Cryst. Solids* 2001; **279**: 136.
- Zahra AM, Zahra CY, Piriou B. *J. Non-Cryst. Solids* 1993; **155**: 45.
- Exarhos GJ. In *Structure and Bonding in Non-crystalline Solids*, Ralfen GE, Revesz AG (eds). Plenum Press: New York, 1986; 203.
- Nelson BN, Exarhos GJ. *J. Chem. Phys.* 1979; **71**: 2739.